Comprehensive energy modeling methodology for battery electric buses

Hussein Basma, Charbel Mansour, Maroun Nemer, Marc Haddad, Pascal Stabat

Title: Comprehensive Energy Modeling Methodology for Battery Electric Buses.

Hussein Basma [a], Charbel Mansour [a,b], Marc Haddad [b], Maroun Nemer [a] and Pascal Stabat [a]

[a] PSL Research University - MINES Paristech, Center for Energy Efficiency of Systems, Palaiseau, France,
[b] Lebanese American University, Industrial and Mechanical Engineering Department, New York, United States of America

Corresponding Author

Hussein Basma

hussein.basma@mines-paristech.fr

5 rue Leon Blum, 91120, Palaiseau, France

Nomenclature

BEB	Battery Electric Bus
APTA	American Public Transportation Association
HVAC	Heating Ventilating and Air Conditioning
EV	Electric Vehicle
SOC	State of Charge
HP	Heat Pump
COP	Coefficient of Performance
EM	Electric Machine
TCS	Torque Control Strategy
RWD	Rear Wheel Drive
BER	Brake Energy Recovery

Abstract

With the announced plans to ban diesel in major European cities from 2025, battery-powered electric buses (BEB) are attracting attention to replace diesel fleets, given their zero tailpipe emissions. However, their large-scale deployment faces several challenges, namely the limited driving range (DR) and the need for adequate charging infrastructure. The limited DR is due to the lower battery specific energy compared to oil-based fuels. Also, the use of electric auxiliaries, especially, air conditioning, reduces the DR further. The DR problem could be resolved either by increasing the battery capacity, which increases the bus cost or by rightsizing the battery alongside an adequate charging strategy to avoid schedule disruption. Therefore, this paper presents a comprehensive energy modeling of a BEB using Dymola, encompassing the different energy systems encountered in BEB. The proposed model serves as a platform to evaluate the bus energy needs during its service to properly size the battery. A powertrain model is presented to emulate the propulsion load. Then, a cabin model alongside a heating ventilating and air conditioning system are developed emulating the thermal load. Finally, auxiliaries necessary for the bus operation are modeled. The energy consumption of each system is assessed under several operating conditions.

1. Introduction

The transport sector contributes almost to a quarter of the global Green House Gas (GHG) emissions and is considered among the most polluting sectors in cities. The contribution of public transportation is around 6%, and the global emissions resulting from heavy-duty vehicles (buses and trucks combined) is expected to increase in the future, despite all improvements in fuel consumption efficiency [1,2]. To that end, several countries are implementing measures for adopting cleaner bus technologies to operate more environmentally-friendly, namely in urban areas [3]. BEB technologies present a promising solution to improve air quality as well as reduce GHG emissions [4]. Their potential CO2 emissions reduction could reach 75%, depending on the electricity generation mix [5–7].

Many challenges are preventing the massive deployment of BEB globally, namely the high capital cost, mainly driven by the cost of the batteries and the cost of the needed electrical

infrastructure. For instance, oversizing the battery capacity to increase the driving range incurs an expensive and unattractive solution for bus operators, especially when compared to diesel buses or other alternative bus technologies [8], not to mention the additional weight carried over by the bus which limits the ridership capacity. On the counterpart, reducing the battery size to limit the bus cost has a direct impact on the charging strategy. It incurs an increase in the charging frequency and power to avoid any schedule disruption at the fleet level, and therefore, increases the cost of the charging infrastructure given the need to install fast-charging technologies and to upgrade in some cases the electrical distribution grid [7,8]. Thus, rightsizing the battery capacity to match the needs of the BEB over the planned daily schedule, along with developing an adequate charging strategy are essential to alleviate the charging load on the electrical grid and to optimize the cost of the bus and the electrical infrastructure.

Rightsizing the battery requires a comprehensive understanding of the BEB energy consumption under the different bus operating conditions, namely the driving patterns, weather conditions, and the variation of the passengers' load during the bus operation. The battery must cover the energy and power needs of the different systems encountered in BEB, being the sole energy and power source on the bus. Those systems include the bus powertrain, the heating ventilating and air-conditioning (HAVC) system required to ensure the passengers' thermal comfort, and other auxiliary systems essential to the bus operation, such as the hydraulic steering system, the pneumatic brakes, the electric lights, and the battery-thermal management system. All these systems present variable but considerable energy consumption during the bus operation; therefore, optimizing the battery size requires a detailed energy assessment of these systems under the different bus operating conditions, such as the weather conditions, driving patterns, and passenger occupancy.

To that end, a detailed and comprehensive energy assessment of BEB is needed considering the different energy systems in BEB.

Several studies have been published over the past decade in the academic literature on assessing the performance of BEB in terms of driving range and energy consumption, as will be reviewed here. Most of these studies focus on quantifying the energy consumption of bus propulsion systems on specific driving cycles, or on evaluating the energy consumption of the HVAC system to maintain thermal comfort inside the bus cabin for given external temperatures.

The majority of the studies focused on improving the driving range of BEB, either by optimizing the consumption of the powertrain at the system level [11] or by enhancing the technology of the powertrain components. These studies presented several approaches to model the powertrain and the components, such as multi-physical models [12] or mathematical models [13,14]. They assessed the propulsion consumption performance under different driving cycles, road topographies, and passengers' load [15,16].

Few studies evaluated the energy consumption derived from operating the HVAC system in electric buses. These studies considered static thermal models to estimate the cabin load [18] and simplified HVAC system models, with no mention of the adopted control strategy, which compromises the consumption accuracy of the model. Besides these studies, some tackled the HVAC system energy consumption for electric passenger vehicles rather than electric buses

[19,20]. Few of them present detailed cabin models, intended to estimate the thermal passenger load [21,22] while others are used to improve the COP of the HVAC system [23,24] or to compare the performance of HVAC to other heating technologies [25].

None of the studies in the literature considered a detailed evaluation of the energy consumption resulting from the use of the auxiliaries of buses. Most of the time, this consumption is considered negligible compared to that of the propulsion system. Among the studies considering these auxiliaries in the model, the load was either assumed constant during the vehicle operation [26] or following a predefined trend [30]. This simplification is mainly observed in studies focusing on the cost assessment of buses [31,32]. Such assumptions could be acceptable for estimating the consumption of passenger vehicles; however, it underestimates the consumption of buses and heavy-duty vehicles, as these auxiliaries are high-energy consumers, namely the battery thermal management system [22]. Therefore, the resulting energy consumption is significant [30, 35], which consequently reduces the BEB driving range.

Based on the above, the following gaps and limitations are identified in the literature:

- None of the studies presents a comprehensive BEB energy model that considers all energy systems encountered in BEB (propulsion, HVAC, and auxiliaries) to assess the resulting cumulative energy consumption.
- Simple cabin and HVAC models were considered in the studies, underestimating the significant consumption of the HVAC system and its impact on reducing the driving range of BEB, in particular, under severe cold and hot weather conditions.
- Similarly, the auxiliaries present considerable energy consumption in buses. Therefore, detailed models of the pneumatic, electric, hydraulic auxiliaries in addition to the battery thermal management system should be considered, taking into account the dynamic load of these auxiliaries under the various bus operating conditions.
- There is no comprehensive assessment of the consumption of each energy system under the different operating conditions of the bus (driving patterns, weather conditions, and bus occupancy).

Therefore, this paper tackles these four identified gaps and limitations in the literature by presenting a comprehensive energy modeling methodology for the different energy systems of an electric bus. Each of the energy systems encountered in BEB and showing a significant impact on the driving range is modeled thoroughly to assess its energy consumption under the different bus operating conditions.

This paper is original in three ways: first, to the authors' best knowledge, it is the only documentation in the literature of a comprehensive methodology to model the BEB energy performance considering all its energy systems as they significantly impact the BEB energy consumption. Second, this paper provides a detailed energy assessment on the impact of driving and weather conditions, and passengers load on the BEB energy consumption and driving range. Finally, the paper presents a tool for bus operators to consider the proper battery sizing and the required charging infrastructure by precisely assessing the BEB energy needs. The methodology is presented in section 2, and the simulation results are illustrated in section 3.

2. Methodology

This section presents the modeling methodology considered in this study. BEB technology is first explained, then the modeling of the bus energy systems is presented: the powertrain, the cabin and HVAC system, and finally, the auxiliaries.

2.1 Bus Configuration and Specifications

A typical BEB configuration is presented in Figure 1.

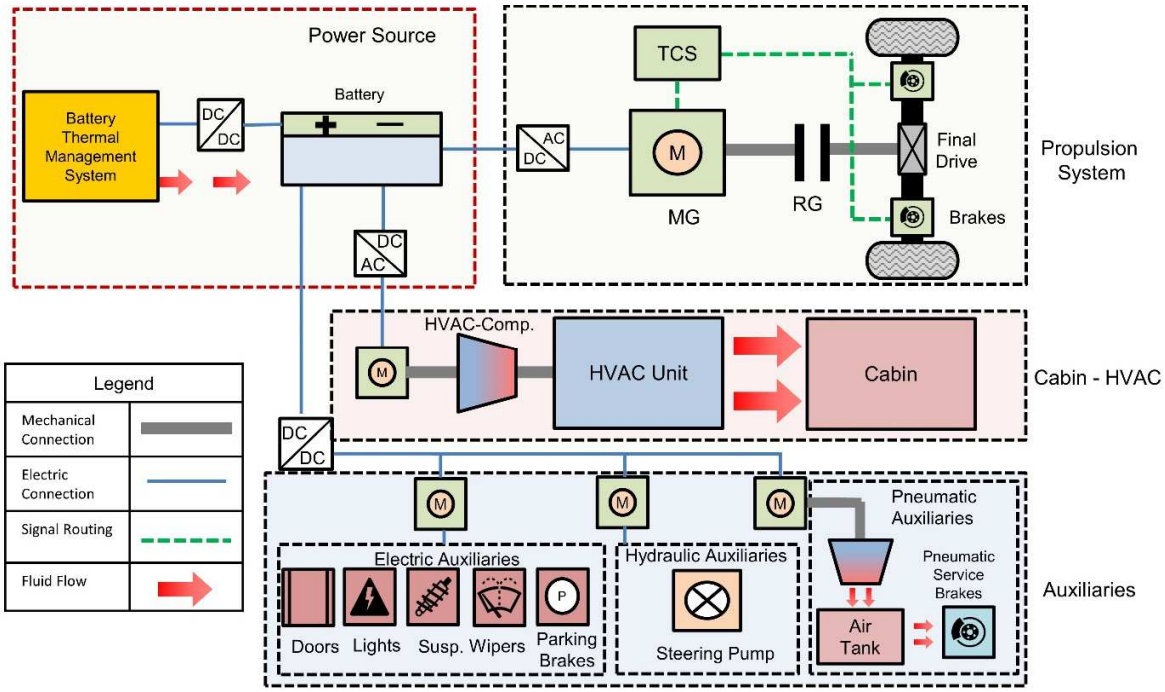

Figure 1: BEB components configuration

The bus powertrain architecture consists of a traction unit, a transmission unit, and a braking system. The traction unit consists of an electric machine, powered by a Lithium-ion battery, and controlled by a torque control strategy (TCS) to ensure traction as well as to recover part of the braking energy. The transmission unit consists of a single reduction gear (RG) and a differential given the high torque capability of the electric machine, and the braking system consists of pneumatic brakes used to dissipate the unrecovered braking energy by the electric machine.

A heat pump (HP) is used to meet the thermal comfort needs of the bus cabin. A dedicated electric motor drives the HP compressor in BEB, which allows more flexibility to control the compressor speed, in contrast to the uncontrolled speed of mechanical compressors in diesel buses, powered by the engine.

The auxiliaries are essential features for the bus operation and consume a significant amount of energy to operate. The technology of these auxiliaries differs depending on bus technology. In BEB, most of these features are electrically operated. These are more energy-efficient compared to hydraulic or pneumatic auxiliaries on diesel buses, as they are decoupled from the engine and

can be controlled separately; however, they require more frequent maintenance [27]. One important auxiliary that is exclusively found in BEB is the battery thermal management system (BTMS). This system is essential at extreme weather conditions to ensure the efficient and safe operation of the battery pack [28].

For illustrative purposes, a single deck 12-m bus is considered in the modeling methodology. The bus has 3 doors and equipped with a 300-kWh battery pack. The bus maximum capacity is 55 passengers weighing 68 kg each on average. The bus maximum allowable passengers capacity is driven by the weight of the battery pack as the EU regulations set the maximum bus payload (battery pack and passengers) at 7.5 tons for 12-m long buses [29]. The BEB characteristics needed for the simulation are summarized in Table 1 [28] [17].

Table 1: Bus chassis parameters

	Parameter	Variable	Value	Unit
Chassis	Glider Mass	M_{Glider}	11600	kg
	Battery pack	M_{Batt}	4200	
	Passenger mass	-	3740	
	Gross Vehicle Weight	M_{Total}	**19540**	
	Frontal Area	A_f	8.2	m^2
	Drag Coefficient	C_D	0.55	-
	Rolling Resistance Coefficient	f_r	0.008	-
Wheels	Wheel Radius	R_{Wheel}	0.48	m
	Wheel Inertia	J_{Wheel}	20.52	$kg.m^2$
	Number of Wheels	n_{Wheels}	4	-

2.2 Powertrain Model

The powertrain is modeled using the Dymola simulation tool, based on Modelica language [30]. Different libraries are used and modified to model the multi-physical complexity of the powertrain system, mainly the *rotational mechanics, translational mechanics,* and *electrical library*. The powertrain model consists of modeling the energy needs of the battery, electric machine, wheels, brakes, and torque control strategy, as detailed below.

2.2.1 *Battery Model*

The battery model is composed of 2 sub-models: (1) Electrical Model and (2) Thermal Model.

Battery Electrical Model

The Lithium-ion battery performance is assessed using the quasi-static Rint equivalent-circuit model, which consists of a voltage source alongside an internal resistance, set in series [31]. The model considers the battery empirical data, such as the voltage and internal resistance of each cell as a function of the battery state of charge (SOC), which are illustrated in Figure 2 [32]. The battery pack configuration consists of 108 parallel modules, with 190 cells placed in series per module. The battery cell parameters are summarized in Table 2 [33]. The resulting battery total

energy is 300 kWh with a 465 Ah total charge capacity and an open circuit voltage range between 600-800 V, which is the current state of the art for electric buses [34]. The battery can operate between 30% and 80% SOC to avoid deep discharge that degrade the battery health and reduce voltage drop at low SOC.

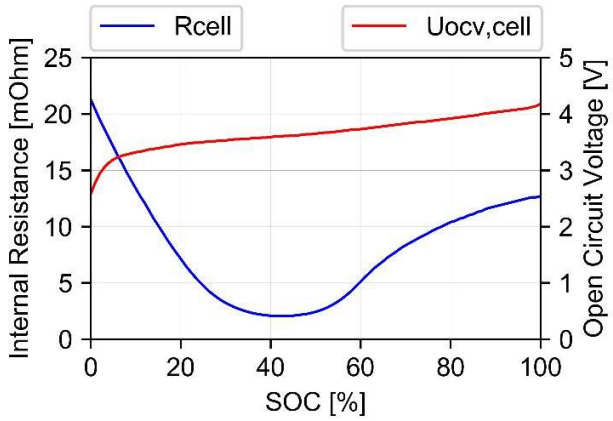

Figure 2: Battery empirical data

Table 2: Battery cell parameters

Parameter	Variable	Value	Unit
Energy Capacity per Cell	E_{Cell}	14.6	Wh
Charge Capacity per Cell	C_{Cell}	4.3	Ah
Mass of a Battery Cell	m_{Cell}	205	g
Number of Parallel Modules	N	108	-
Number of Series Sets	M	190	-

Equation set (1) determines the battery pack parameters for the given configuration, such as the open-circuit voltage (U_{OCV}), total internal resistance (R_{eq}), maximum charge capacity (C_{Max}), maximum energy capacity (E_{Max}), and total mass (M_{Batt}) of the battery pack.

$$\begin{cases} U_{OCV} = M \,.\, U_{OCV,Cell} \\ R_{eq} = R_{Cell} \cdot \dfrac{M}{N} \\ C_{Max} = N \,.\, C_{Cell} \\ E_{Max} = N \,.\, M \,.\, C_{Cell} \\ M_{Batt} = N \,.\, M \,.\, m_{Cell} \end{cases} \quad (1)$$

Equation set (2) determines the battery terminal voltage (U_T), electric current (I_{Batt}), and SOC. This simplified battery model presents an adequate trade-off between complexity and accuracy [35], which made it widely used in modeling electrified powertrains [12,17,36,37].

$$\begin{cases} U_T = \frac{1}{2}(U_{OCV} + \sqrt{(U_{OCV}^2 - 4.P_{Batt}.R_{eq})} \\ I_{Batt} = \frac{P_{Batt}}{U_T} \\ SOC\ (t) = \frac{C_0 - \int_0^t I_{Batt}(t)\,.dt}{C_{Max}} \\ P_{Batt} = \sum P_i\ \forall\ energy\ system\ i \end{cases} \quad (2)$$

Battery Thermal Model

A battery thermal model is developed with its cooling unit to assess the additional energy consumption resulting from the battery thermal management system. A two-state model is used to capture the lumped thermal dynamics of a cylindrical battery in a similar approach to [38,39]. In Figure 3, a scheme of the battery pack thermal model is presented.

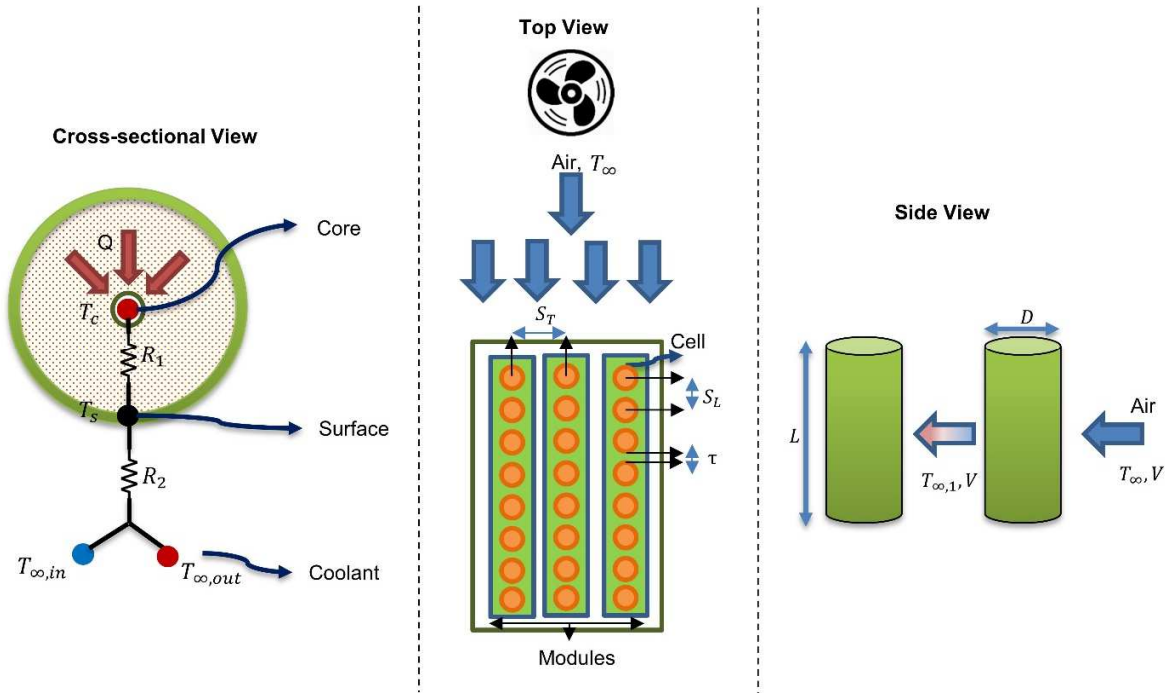

Figure 3: Schematic of the battery pack

The cross-section view shows the two thermal nodes considered in this modeling approach: (1) cell core at temperature (T_C) where heat (Q) is generated internally in the cell and (2) cell surface at temperature (T_S) which is in contact with the coolant at temperature (T_∞). The coolant temperature varies from one cell to another as it gets heated after cooling a certain cell. Thus, this approach considers the difference in temperatures among the different battery cells. R_1 is the conductive thermal resistance between the cell core and surface, and R_2 is the convective thermal resistance between the cell surface and the coolant. Equation set (3) describes the governing

equations of T_C and T_S, where C_c and C_S are the heat capacities of the core and the surface, respectively.

$$\begin{cases} C_c \dfrac{dT_c}{dt} = Q + \dfrac{T_s - T_c}{R_1} \\ C_s \dfrac{dT_s}{dt} = \dfrac{T_\infty - T_s}{R_2} - \dfrac{T_s - T_c}{R_1} \end{cases} \tag{3}$$

The internal heat generation Q is a byproduct of the chemical reactions taking place in the electrode assembly during battery operation [40]. The internal heat generation is governed by equation (4), which accounts for both resistive and entropic heat generation ($\partial U/\partial T$) but neglecting the chemical reaction heat [41].

$$Q = I_{Batt}(U_T - U_{OCV}) + I_{Batt}.T_C.\frac{\partial U}{\partial T} \tag{4}$$

The value of R_1 is obtained experimentally, and it ranges between 3.2 – 3.3 K/W [40].

Equation set (5) determines the value of R_2 depending on the coolant flow characteristics where A_s is the cell surface area, h_{air} is the heat transfer coefficient, D is the diameter of the cell, K_{air} is air thermal conductivity, ν_{Air} and μ_{Air} are air kinematic and dynamic viscosities respectively, Cp_{Air} is air specific heat capacity at constant pressure, Re is Reynold's number, Pr is Prandtl's number, Pr_s is Prandtl's number evaluated at the surface of the cell, N_u is Nusselt's number and finally m and c are geometric parameters and V is the maximum air speed near the cells.

$$\begin{cases} R_2 = \dfrac{1}{A_s.h_{air}} \\ h_{air} = \dfrac{Nu.K_{air}}{D} \\ N_u = 0.97.c.Re_D^m.Pr^{0.36}.\left(\dfrac{Pr^{\frac{1}{4}}}{Pr_s}\right) \\ V = \dfrac{\dot{m_{air}}}{\rho_{air}.A_c}.\dfrac{S_T}{S_T - D} \end{cases} \tag{5}$$

Battery Thermal Management System

The Battery Thermal Management System (BTMS) is composed of 2 components: (1) the cooling unit and (2) the cooling unit controller.

Applications with very high energy density, such as Lithium-ion batteries, require active air cooling as it is capable of achieving a good compromise between adequate cooling and system complexity [42]. In this study, the fan model FB020-2E is used which can supply air to cool the battery cells from three different air sources: (1) ambient air, (2) bus cabin air, (3) cooled air

using an evaporator that is connected to the main HVAC unit. The used fan can supply up to 1000 CFM and 100 Pa static pressure. The resulting air speed around the cylinder is between 6-8 m/s. The fan's flow rate, static pressure and power consumption data are given in [43]. The cooling unit consumes electric energy directly from the battery.

The cooling unit controller should ensure that the battery cell core temperature is within the desired operating range of 20 – 35 °C [44]. This is achieved through active cooling with three operating modes depending on the ambient conditions. Cabin air cooling is activated for ambient temperatures between 20-35 °C or temperatures less than 10 °C while ambient air cooling is activated between 10-20 °C and refrigerant cooling for temperatures above 35 °C. The total power demand of the battery cooling unit is modeled with the HVAC unit.

2.2.2 *Electric Machine Model*

The electric machine (EM) is modeled using the static efficiency map, including the efficiency of the inverter, as a function of the torque (T_{EM}) and speed (ω_{EM}) illustrated in Figure 4, and inertial components to capture the machine's dynamic performance during both propulsion and brake energy recovery. Note that this brake power recovery is limited by the maximum power of the machine and the battery maximum charging power. The EM torque is controlled by the TCS.

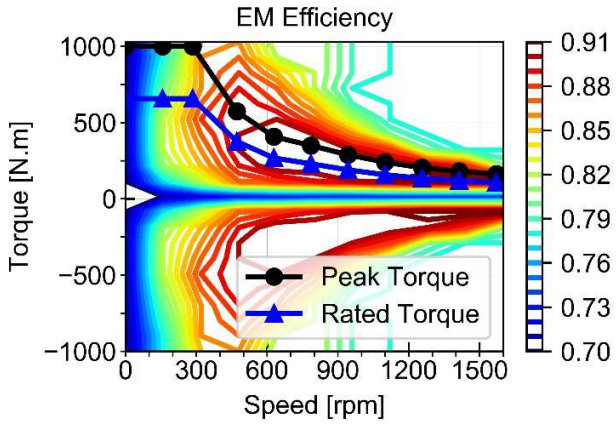

Figure 4: Electric Machine efficiency map

Equation set (6) determines the EM performance parameters, namely the electric current (I_{EM}) and the mechanical ($P_{EM,mech}$) and electrical power ($P_{EM,elec}$) of the machine. Note that η_{EM}^{k} is the EM efficiency where k takes the value of -1 during traction and 1 during braking.

$$\begin{cases} P_{EM,mech} = \omega_{EM}.T_{EM} \\ P_{EM,elec} = P_{EM,mech}.\eta_{EM}^{k} \\ I_{EM} = \dfrac{P_{EM,elec}}{U_T} \end{cases} \quad (6)$$

2.2.3 *Wheels and Braking System Model*

A rear-wheel-drive (RWD) bus is considered with two front wheels and two rear wheels. During traction, the transmission system transmits the traction torque from the EM to the rear wheels.

Two modes of braking are used, mechanical braking and regenerative braking through brake energy recovery. The choice of the braking mode is controlled by the TCS discussed in the next section

To simplify the equations, the two front wheels are combined into one ($T_{W,Front}$) and the two rear wheels are combined into one as well ($T_{W,Rear}$). Equation set (7) shows the wheels' torque equations with i_{RG} the reduction gear ratio, i_{FD} the final drive ratio, $T_{Rear,Br}$ the rear wheels mechanical braking torque, and T_{Reg} the regenerative braking torque.

$$\begin{cases} \begin{cases} T_{W,Front} = 0 \\ T_{W,Rear} = T_{EM}.i_{RG}.i_{FD} \end{cases} & \text{Traction} \\ \begin{cases} T_{W,Front} = T_{Front,Br.} \\ T_{W,Rear} = T_{Rear,Br.} + T_{Reg} \end{cases} & \text{Braking} \\ F_{Wheel} = \dfrac{T_{W,Rear}}{R_{Wheel}} & \text{Total Force} \end{cases} \tag{7}$$

2.2.4 *Torque Control Strategy*

The TCS in electric powertrains must ensure that the driver torque demand, communicated through the acceleration and brakes pedal, is always met. The driver is modeled using a proportional integral derivative controller (PID) that follows a reference velocity profile defined by the driving cycle. The PID outputs the required torque to follow the reference speed. The TCS receives the driver torque to control the EM propulsion and braking torques accordingly. During traction, the TCS controls the EM torque to be equal to the driver torque demand respecting its maximum torque limitation. However, during braking, the TCS controls the mechanical braking torque depending on the regenerative braking torque imposed by the EM and the driver torque demand, while respecting the EM maximum regenerative torque capacity and the battery maximum SOC.

Finally, the power unit and the powertrain components are sized to meet public transit performance specifications set by the American Public Transportation Association (APTA), as in [45]. The sizing of the components is summarized in Table 3.

Table 3: Summary of the components sizing

BEB	Battery	Maximum Capacity	300 $\boldsymbol{kWh}$
	Electric Machine	Rated Power	135 kW
		Maximum Continuous Torque (Rated Torque)	650 $N.m$
		Maximum Transient Torque (Peak Torque)	1000 $N.m$

	Transmission	Reduction Gear Ratio	5.5
		Final Drive Ratio	5

2.3 Cabin - HVAC System Model

2.3.1 *Cabin Model*

The thermal load for heating/cooling the cabin in a BEB should be assessed to better understand its impact on the BEB driving range, given the significant incurred energy consumption. A vehicle cabin thermal model is developed by the current co-author in [21] for an electric vehicle (EV). The cabin model consists of four main sub-models: (1) cabin interior, (2) cabin walls, (3) passengers, and (4) cabin internal materials. This model estimates the temperature of the cabin.

The cabin interior is modeled as a single thermal node using a mono-zonal approach that considers both the transient and steady-state phases, which is a convenient energy assessment methodology for the thermal load in EV [26].

The wall sub-model is an array of walls representing the bus body (Top, bottom, two sides, front, and back). The walls are either opaque or glazing, and the bus geometry determines the total areas of these two wall types. Each wall has two sides, an outer side facing the environment and an inner side facing the cabin interior. Through the walls, six modes of heat exchange are considered in this model: (1) convection with the exterior, (2) conduction through the wall, (3) convection with the cabin interior, (4) incident radiation, (5) transmitted and (6) absorbed radiation through glazing.

As for the passengers' sub-model, each passenger is modeled as a constant source of heat rejection (70 W per person). Finally, the cabin internal material sub-model is a thermal node with specific heat capacity and geometry that interacts with the cabin interior through convection and radiation.

Besides, during a daily bus operation, doors opening has a considerable influence on the interior temperature due to the frequent opening of the doors. These energy losses are considered in the modeling by adding a variable heat flow rate in/out of the cabin, which depends on the ambient temperature, bus cabin temperature, and the duration of open-doors [46]. A more detailed description of the cabin model is presented in [21].

2.3.2 *HVAC Model*

The complete HVAC unit consists of 2 reversible heat pumps, an air circulation system, and the battery thermal management system. Figure 5 introduces the HVAC unit scheme.

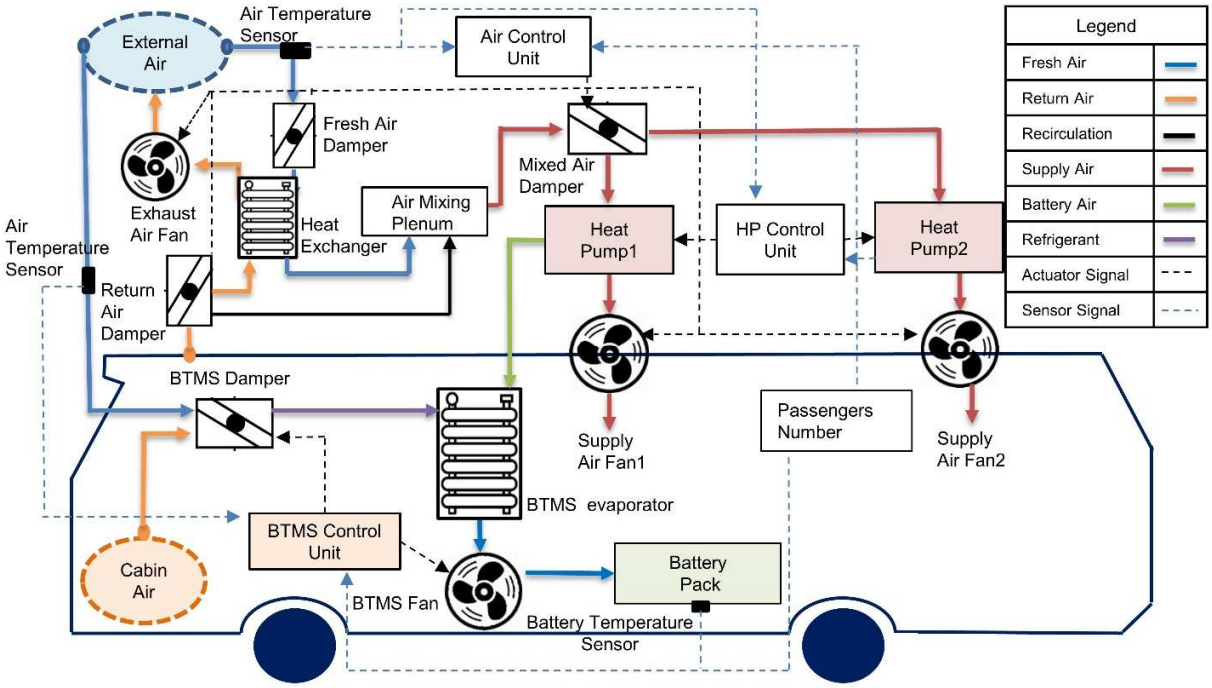

Figure 6: HVAC Unit Scheme

- **Reversible Heat Pump**

Thermal load calculations for a bus of similar specifications show that the maximum required heating capacity is around 35 kW [18]. In BEB, the use of multiple HPs is common as there are many buses equipped with more than 1 HP. 2 reversible HPs are considered in this study, each rated at 20 kW, and placed at the middle and the back of the bus. A more detailed description of the heat pump model is presented in a previous study [47].

- **Air Circulation System (ACS)**

The air circulation system (ACS) is mainly composed of a set of fans, dampers, and mixers. As shown in Figure 5, two air supply fans provide heated/cooled air to the cabin, one exhaust air fan that discharges air from the cabin and two fans (masked inside the HP block) to draw fresh air from the exterior. Also, a set of dampers is used to regulate the airflow. Part of the exhaust air flows through an air-air heat exchanger where the fresh air flow recuperates part of the remaining exhaust air energy. Air properties are calculated as shown in equation (8), where T refers to temperature, w refers to absolute humidity and rec refers to the air recirculation rate.

$$\begin{cases} T_{air}^{mix} = (1 - rec).T_{air}^{fresh} + rec.T_{air}^{cabin} \\ w_{air}^{mix} = (1 - rec).w_{air}^{fresh} + rec.w_{air}^{cabin} \end{cases} \quad (8)$$

- **Battery Thermal Management System**

The final component of the HVAC system is the battery thermal management system (BTMS). It is composed of a fan, an evaporator, and air dampers to determine the air source (cabin, exterior, or conditioned exterior/cabin air). An electric resistance heater is also used to heat the freezing air during winter.

Finally, the total power consumption of the HVAC unit is the sum of power needed to operate the two HP, the ACS and the BTMS, as shown in equation (9) with P_{HVAC} as the total HVAC unit power demand, $W_{comp.}$ the compressor work, P_{fans} the ventilation fans power consumption, $P_{resistance}$ the electric resistance heater power consumption and η_{em} the efficiency of the EM driving the HVAC unit.

$$P_{HVAC} = \frac{W_{comp.} + \sum P_{fans}}{\eta_{em}} + P_{resistance} \tag{9}$$

- **Control Scheme**

The default HVAC controllers in buses are known by the ON-OFF controllers. The control strategy aims at maintaining the cabin temperature at the desired value within certain low and high limits by controlling the compressor speed. In this study, an ON-OFF controller is used to attain thermal comfort conditions inside the bus cabin between 19-23 °C. Maximum blown air temperature and minimum fresh air flow rate are determined considering passengers' comfort inside the bus, as shown in [45]. The required amount of fresh air is dependent on the number of passengers inside the BEB. Four levels of passenger occupancy are defined in the HVAC unit controller (very low: < 10 passengers, low: < 25, medium: < 40 and high: > 40).

2.4 Auxiliaries' Model

2.4.1 *Electric Auxiliaries*

The electric auxiliaries in BEBs are modeled as a power demand directly from the battery whenever actuated. The model receives the driver's commands to actuate these auxiliaries. These power demands are quantified as in [48] and shown in Table 4. The total electric AUX power consumption is shown in equation (10) where η_{em} is efficiency of the auxiliary electric motor.

$$P_{Ele} = \frac{P_{Doors} + P_{PB} + P_L + P_W}{\eta_{em}} \tag{10}$$

Table 4: Electric Auxiliaries Power Demand

	Variable	Value	Unit	Process Duration [sec]
A pair of Doors opening and closure	P_{Doors}	90	W	3
Parking Brakes Activation	P_{PB}	560	W	1
Lighting System	P_L	500	W	-
Wipers	P_W	110	W	-

2.4.2 *Hydraulic Auxiliaries*

The main hydraulic AUX in a bus are the steering pump and the suspension system. The steering pump must always provide the required hydraulic pressure in the bus steering system. The power consumption of the steering pump can be characterized function of the bus speed as in [48].

The suspension system is responsible for kneeling and lifting the bus front at the stops. This feature aims at easing passengers' entrance and exit to/from the bus. A hydrostatic system is used to lift the bus using pressurized liquid. The height of the bus floor changes by (Δh = 65 mm) for the considered bus. Equation (11) describes the suspension system power consumption. M_{Front} is the bus front weight which corresponds to the mass of the front axle and the mass of the chassis supported by the front axle. In addition, it is assumed that the weight of 1/3 of the passengers is supported by the front axle based on the bus geometry. The suspension system efficiency $\eta_{Susp.}$ is considered constant and equals to 70% and Δt represents the duration of the lifting process taken to be 3 seconds [48].

$$\begin{cases} P_{Susp.} = \dfrac{M_{Front}.g.\Delta h}{\eta_{Susp.}.\Delta t} \\ P_{Hyd} = P_{pump} + P_{Susp.} \end{cases} \tag{11}$$

2.4.3 *Pneumatic Auxiliaries*

The pneumatic system mainly operates the service brakes of the BEBs. Pneumatic brakes (Air Brakes) are friction brakes that use the energy stored in compressed air at 10 bars approximately to press the pistons, so they apply the needed pressure on the brake pads to decelerate the bus. The pneumatic system in BEB is formed of a compressor, air tank to store compressed air, an electric machine to drive the compressor, and a foot valve that regulates the airflow.

Equation (12) describes this flow rate ($\dot{V}_{air}^{Br.}$) function of the driver's braking torque ($T_{Dr,Br.}$), the maximum braking torque ($T_{Br.Max}$) and the maximum airflow rate through the valve ($\dot{V}_{air,max}^{Br.}$). The valve can supply up to 4 L/s of compressed air at 10 bars.

As the most essential safety feature, the pneumatic system should always be capable of supplying enough compressed airflow to operate the service brakes as required. For this sake, it is essential to monitor the level of compressed air inside the air tank as shown in equation (12) where ($\dot{V}_{air}^{comp.}$) is the compressor volumetric flow rate to the air tank.

An ON-OFF buffer controller controls the compressor to ensure that the air tank volume is always maintaining a minimum level of compressed air at 10 bars. This minimum threshold is set to be 50% of the maximum air tank volume. When the air tank volume drops below 50% of its maximum volume, the compressor is turned ON at maximum speed until the air tank is full where it can provide 240 L/min of compressed air consuming 2.7 kW. The electric motor driving the compressor operates at a fixed speed and constant efficiency of 80%. The pneumatic AUX power consumption is expressed in equation (12) as well.

$$\begin{cases} \dot{V}_{air}^{Br.} = \dfrac{T_{Dr,Br.}}{T_{Br.Max}} . \dot{V}_{air,max}^{Br.} \\ V_{air}^{Tank}(t) = V_{air}^{Tank}(0) + \displaystyle\int_0^t \left(\dot{V}_{air}^{comp.} - \dot{V}_{air}^{Br.}\right). dt \\ P_{Pneu} = \dfrac{P_{Comp.}}{\eta_{em}} \end{cases} \quad (12)$$

3. Simulation Results and Discussion

This section utilizes the proposed model to simulate the bus energy consumption at different operating conditions. These operating conditions are the driving conditions, weather conditions, and passengers' load. Driving conditions are the bus velocity profile, driving behavior, trip distance and duration, road topography, and the number of stops along the route. These driving conditions affect the energy behavior of the BEB. On the other hand, weather conditions such as temperature impacts the bus thermal needs only and thus affect the HVAC unit energy consumption. Moreover, the passengers' load influences the energy consumption of the bus due to the additional weight on-board and the varying thermal comfort conditions depending on the number of passengers occupying the bus.

3.1 Impact of Driving Conditions

The BEB model is simulated at all drive cycles presented in Table 5 each representing specific driving conditions in terms of traffic levels, driver's behavior, and route type (urban or intercity route depending on the number of stops per km). Weather conditions and passengers' load are held constant across the different simulations at this stage where external temperature is set to 20°C, and the passengers' load is 30 passengers (60% occupancy rate).

Table 5: Drive cycles specifications

Cycle Name	Cycle ID	Duration [sec]	Distance [km]	Average Speed [km/h]	Average Deceleration [m/s^2]	Idle Time [s]	Number of Stops
New York Bus	NYB	600	1.113	5.93	0.163	404	12
Manhattan Bus	MB	1089	3.32	10.98	0.188	395	21
New York Composite	NYC	1029	4.5	14.1	0.19	341	19
Orange County Transit Authority	OCTA	1909	11.845	19.84	0.237	407	31
Central Business District	CBD	569	3.64	20.43	0.2478	122	14
City Suburban Heavy Vehicle	CSHV	1780	12.1	21.86	0.167	385	19
Braunschweig	BRAU	1740	12.23	22.4	0.241	442	29

Urban Dynamometer	UDDS	1369	13.48	31.51	0.2248	259	17
Arterial	ART	291	3.6	39.71	0.276	48	4
Commuter	COM	329	7.248	70.28	0.82	40	1

Figure 6 illustrates the propulsion system energy consumption at the different simulated driving conditions for the bus configuration presented in section 2.1 and the battery size of 300 kWh. The figure shows the energy consumed during the bus acceleration mode, BER mode, and the resulting total propulsion energy consumption, which is the sum of the 2 mentioned energy entities. The data labels shown in the figure correspond to the total propulsion energy consumption.

The propulsion system energy consumption witnesses high variations at the different simulated driving conditions. The highest energy consumption is recorded during the NYB drive cycle at 2.62 kWh/km, whereas the lowest value is recorded during the CSHV drive cycle at 1.7 kWh/km, which represents a 35% reduced energy consumption.

The main reason behind this variation is related to the drive cycle average speed. In Figure 6, the drive cycles are sorted by ascending order of their average velocities. At higher average speeds, the energy consumption decreases. This indicates that with more substantial traffic, resulting in lower average speeds, the propulsion system energy consumption increases. When more frequent starts and stops are encountered, the EM does not operate at steady-state conditions resulting in additional consumption due to frequent accelerations reducing its efficiency.

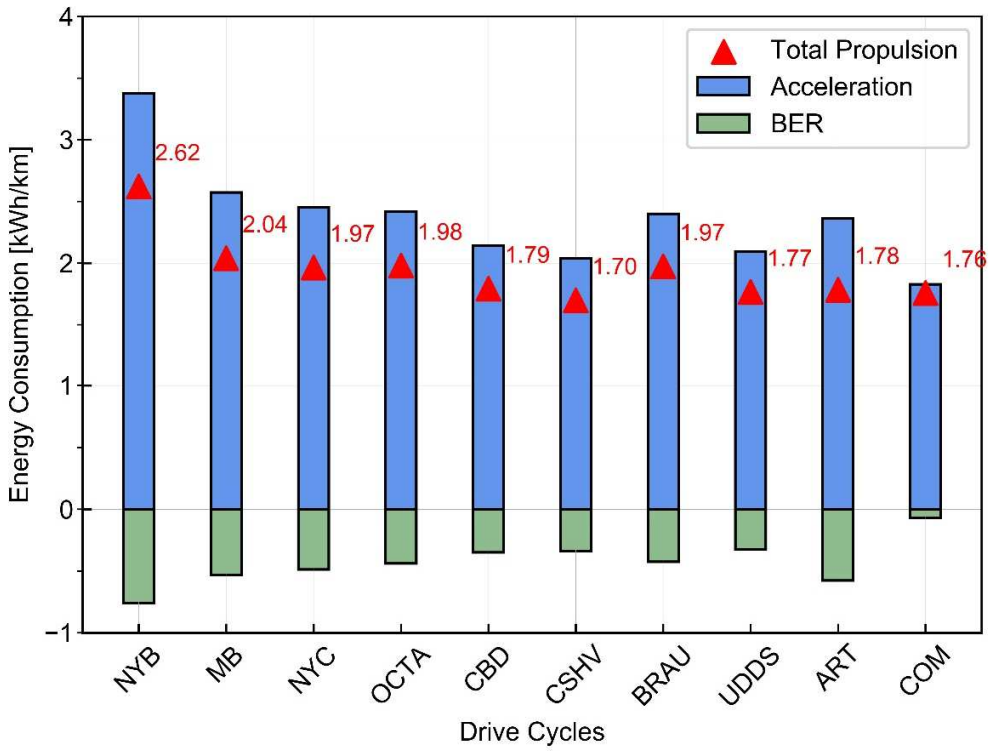

Figure 6: Propulsion system energy consumption at different driving conditions

The presented analysis shows the impact of traffic conditions and route specification on the propulsion system energy consumption. Buses consume more energy along routes that encounter high levels of traffic such as urban buses or city center buses. In contrast, buses operating along routes with fewer traffic levels benefit from reduced energy consumption, which is the case for intercity buses for example.

Similar to the propulsion system, the auxiliaries' energy consumption is varying under the different driving cycles. The energy consumption partitions among the different auxiliaries are illustrated in Figure 7. The air compressor and the steering pump are the main energy consumers, followed by the suspension system and finally, the doors and the parking brakes representing the electric system. BTMS energy consumption is negligible as this simulation is conducted at 20 °C and it does not show any variation with the varying driving conditions; thus, it is not presented in the figure.

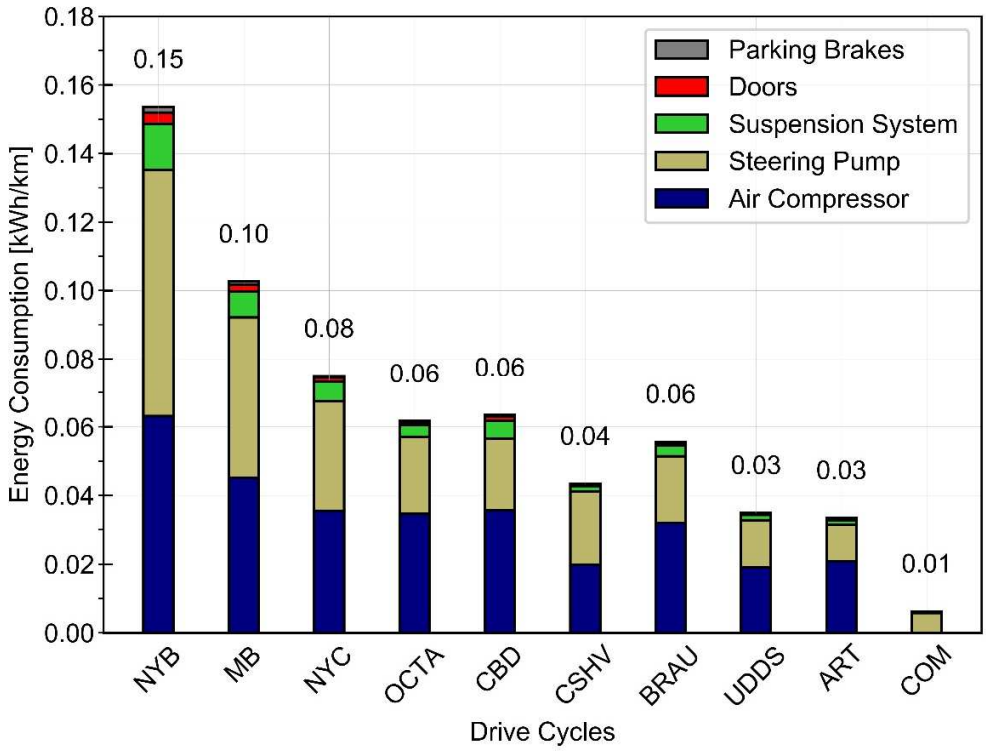

Figure 7: Auxiliaries' energy consumption at different driving conditions

The auxiliaries' energy consumption is highly affected by the different driving conditions, especially the air compressor and the steering pump. The total auxiliaries' energy consumption can represent up to 6% (NYB and MB) of the total BEB energy consumption.

The steering pump power consumption is directly related to the bus speed. The higher the driving cycle average speed is, the lower is the steering pump energy consumption. Once again, heavy traffic conditions increase another auxiliary feature energy consumption up to 3 times compared to lighter traffic conditions.

The main pneumatic auxiliary in a BEB is the service brakes, powered by the air compressor. The latter is directly affected by the frequency and power of braking encountered during the trip. The higher the driving cycle average deceleration, the higher is the air compressor energy consumption. In other words, heavy traffic conditions associated with high decelerations can increase the pneumatic system energy consumption in a BEB by 50% when compared to bus standard traffic conditions (considered in this study to be the MB and NYC driving cycles). With more deceleration, more compressed air is needed to actuate the service brakes, and thus, the air compressor is turned on more frequently, resulting in increased energy consumption. Driving conditions with high levels of traffic and deceleration are mainly encountered in urban areas and inside city centers resulting in this additional energy consumption.

The main electric auxiliaries in BEB are the doors and the parking brakes. In addition to the suspension system, these auxiliaries are only actuated when the bus stops, and it is noteworthy to

mention that the number of stops differs from one driving cycle to another. The higher the number of bus stops per km, the higher is the energy consumption. The cycle with the highest number of stops per km (NYB) records the highest energy consumption with a 100% increase when compared to bus standard traffic conditions (MB and NYC cycles). The number of bus stops per km is related to the route specifications as the number of stops will increase in urban areas and inside city centers resulting in additional energy consumption.

3.2 Impact of Weather Conditions

The BEB model is simulated at a variety of weather conditions. The external temperature ranges between -10 °C and 40 °C as they represent the extreme temperatures encountered in the city of Paris throughout the year. Driving conditions and passengers' load are held constant across the different simulations where the MB drive cycle is used, and the passengers' load is fixed at 30 passengers (60% occupancy rate).

Figure 8 shows the HP compressor average electric power consumption at different external temperatures.

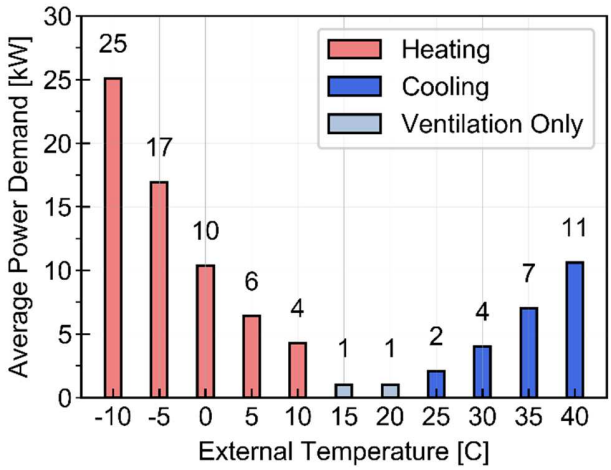

Figure 8: HVAC unit average electric power consumption at different external temperatures

The HVAC unit average power demand is the highest at extreme weather conditions due to the high thermal load at these conditions. In addition, the HVAC system COP at extreme conditions is very low, which further deteriorates the HVAC unit performance at these conditions. The average power demand decreases gradually as external temperatures approach room temperature. Between 15 – 20 °C, neither heating nor cooling is required, and the slight power consumption (around 1 kW) is due to the ventilation fans. At extreme weather conditions, the HVAC unit energy consumption is equal to the propulsion system energy consumption.

In addition to the HVAC unit power demand, the variation in external temperatures affects the BTMS power demand. Figure 9 shows the BTMS average electric power demand at different external temperatures.

At extreme weather conditions, the BTMS average power demand is the highest as the air used to cool down the battery cells requires cooling during extremely hot conditions and heating during extremely cold conditions. The BTMS average power demand can reach 6 kW at extreme hot conditions, which constitutes one-third of the total HVAC unit power demand.

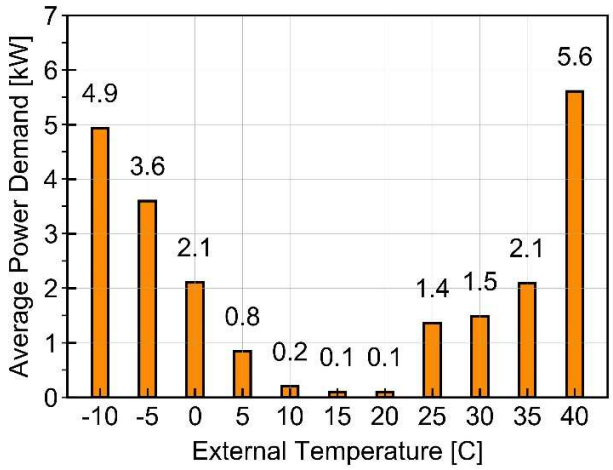

Figure 10: BTMS average electric power demand at different external temperatures

3.3 Impact of Passengers' Load

In this section, the impact of the bus passenger occupancy on energy consumption is presented. The BEB model is simulated under four levels of bus occupancy as presented in section 2.3.2 and summarized here (very low: < 10 passengers, low: < 25, medium: < 40 and high: > 40). The simulations are carried out under the same driving conditions, represented by the MB driving cycle, and under two weather condition cases, illustrated by two external temperatures (0 °C to emulate a cabin heating scenario and 30 °C to emulate a cabin cooling scenario).

Figure 10 shows the HVAC unit average electric power demand during transient and steady states for different levels of passengers' occupancy. Under the heating scenario at 0 °C, the average power demand slightly increased from 10.5 kW to 11.1 kW between the minimum and the maximum passengers' loads, which represents a 5 % increase in the power demand. On the other hand, when considering the cooling scenario at 30 °C, the average power demand drastically increased from 2.9 kW to 6 kW, which represents a 100 % increase in the power demand. The results show that the change in the average power demand is less sensitive to the increase of bus occupancy under the heating scenario as compared to the cooling scenario. This is because with higher passengers' load, more heat is rejected into the bus cabin from the passengers, and thus, it helps in heating the cabin and reducing the heating needs, unlike cooling where this factor contributes adversely and increases the cooling needs.

It is noteworthy to mention that the illustrated average power demand of the HVAC system increases by steps as a function of the passengers' occupancy. This is due to the adopted control strategy of the HVAC system, which adjusts the control variables of the system according to the four defined levels of passengers' occupancy.

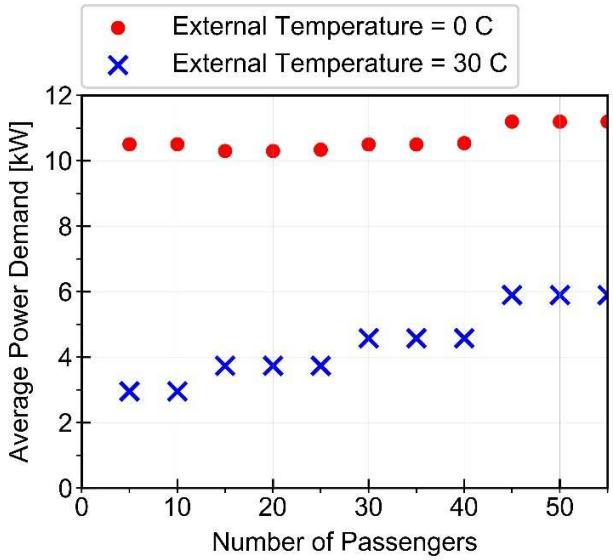

Figure 10: HVAC unit average electric power demand at different passengers' load

In addition to its impact on the HVAC power demand, increasing the passengers' load presents an impact on the propulsion system energy consumption. This consumption could increase by more than 15% with a full bus occupancy when compared to an empty bus.

The energy consumption/power demand at varying operating conditions of each energy system encountered in a BEB is summarized in Figure 11. Panel (a) shows the propulsion system energy consumption as function of the BEB average speed and the number of passengers occupying the bus. The propulsion system energy consumption is the highest at low average speeds and high passengers' occupancy exceeding 2.4 kWh/km. This value gradually decreases at higher average speeds and lower passengers' occupancy reaching 1.7 kWh/km representing a 35% reduction in propulsion system energy consumption.

Panel (b) shows the HVAC unit average power demand at different external temperatures and passengers' occupancy. The HVAC power demand is the highest at extreme weather conditions (-10 °C and 40 °C). For extreme cold conditions (-10 °C), at low passengers' occupancy, the HVAC power demand exceeds 30 kW, however, as a higher number of passengers occupy the bus, this value slightly decreases reaching 25 kW for the highest BEB passengers' occupancy. This is due to the relatively lower heating needs at higher passengers' occupancy resulted from the higher heat rejection by passengers. On the contrary, the HVAC power demand at extreme hot conditions (40 °C) increases with higher passengers' occupancy as the heat rejected by the passengers increases the BEB cabin required thermal load.

In panel (c), the AUX average power demand is presented at different average speeds and average deceleration. Lower average speeds increase the AUX power demand mainly due to deterioration in the hydraulic pump efficiency at low speeds. Furthermore, higher decelerations during the BEB trip increase the pneumatic system energy consumption and thus increasing the total AUX power demand.

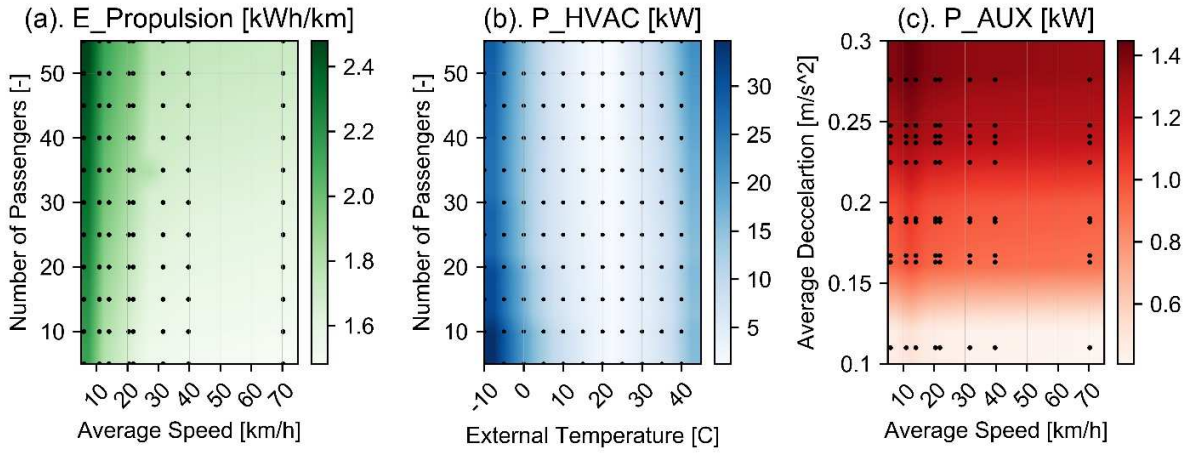

Figure 11: Energy consumption/power demand of each energy system at the varying operating conditions

Finally, the BEB energy consumption is summarized in Figure 12, summing-up the energy consumed by each of the energy systems under the assessed operating conditions, for three levels of bus occupancy (full occupancy, 50% occupancy, and 10% occupancy). The driving patterns are represented in the figure by the bus average speed, and the weather conditions are represented by the external temperature. The energy consumption data presented in Figure 12 are checked against typical real-world working conditions for bus line number 21 in the city of Paris. The obtained energy consumption results are comparable.

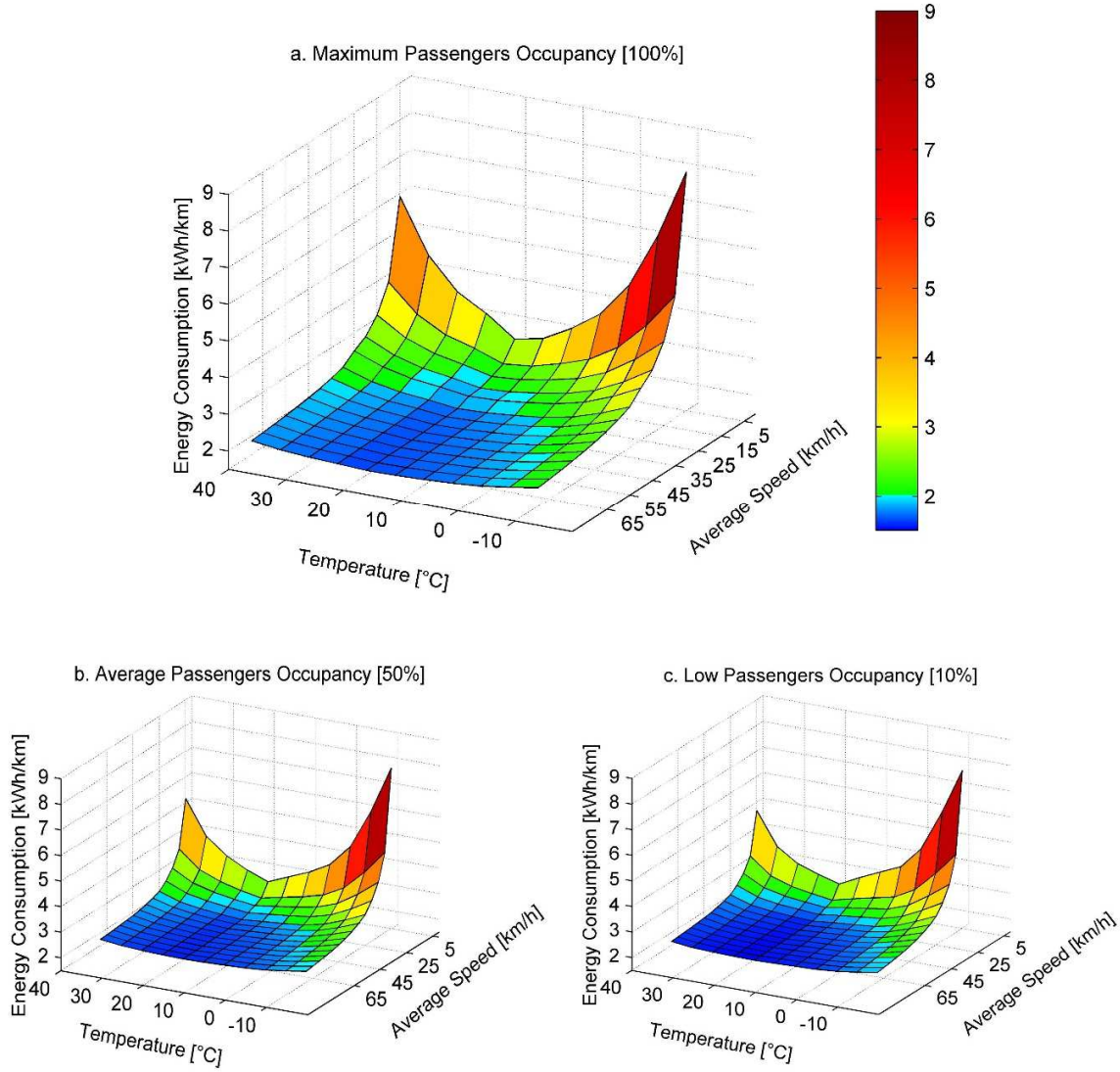

Figure 12: Variation of BEB energy consumption at different operating conditions, (a) maximum occupancy, (b) 50% occupancy, (c) 10% occupancy.

The total BEB energy consumption under standard driving patterns of 15-25 km/h and moderate weather conditions with temperatures between 15-25 °C ranges between 2-3 kWh/km for the case of maximum passenger occupancy. Under these conditions, the propulsion system contributes to approximately 80% of the total energy consumption, followed by the HVAC system with 14% and 6% for the auxiliaries, including the BTMS.

This total energy consumption increases when the bus average speed decreases or when external temperatures deviate from the thermal comfort temperature range of the bus cabin (estimated at 19-23°C during winter and 23-27°C during summer). For example, the total energy consumption of a BEB drastically increases to 8 kWh/km at extreme external temperatures (-10 °C, 40 °C) and

low average speeds (5-10 km/h). Under these conditions, the consumption share of the HVAC system increases to 58% out of the total BEB energy consumption, followed by 29% for the propulsion system and 13% for the auxiliaries and the BTMS.

This observed high energy consumption is the result of 2 factors, (1) the high power demand of the HVAC system for heating/cooling under these extreme temperatures, and (2) the low bus average speed which leads to prolonged trip durations, with the HVAC system operating at high power.

Figure 12 (b) and (c) illustrate the total energy consumption for 50% and 10% of passenger occupancy, respectively. The figure shows similar behavior to the high energy consumption under extreme cold and hot temperatures and low bus average speed. However, the magnitude of the total energy consumption decreases with fewer passenger occupancy, mainly due to the decrease in the BEB total weight, which reduces the propulsion system energy consumption. Also, the HVAC energy consumption decreases in this case, as the ventilation requirements are reduced for lower levels of passenger occupancy; therefore, less energy is consumed to heat/cool the fresh ventilated air.

The significant increase in BEB energy consumption at extreme operating conditions reduces the BEB driving range drastically. For instance, city buses that operate with average speeds below 10 km/h and in extremely cold/hot climate conditions are subjected to a severe reduction in their driving range. This may affect their operation during the day by creating schedule disturbances due to the limited battery energy capacity.

4. Conclusion and Future Work

This paper provides a detailed energy modeling methodology to assess the energy consumption of BEB. The proposed model considers the different energy systems encountered in BEB, such as the propulsion system, HVAC system, and auxiliaries. The model integrates all these energy systems into a single platform to better assess the total bus energy consumption. A detailed powertrain propulsion model is introduced to assess the energy consumption due to propulsion. An electric vehicle cabin model is adapted to fit a bus application, and an HVAC unit model is presented to assess the heating and cooling needs of the bus. Moreover, a dynamic model that introduces the different auxiliaries in BEB, such as the pneumatic, hydraulic, electric, and battery thermal auxiliaries is presented as well.

Different simulations are conducted using the proposed models to study the behavior of the different energy systems across the different operating conditions. The impact of driving conditions on the bus's energy consumption is presented. Heavy traffic conditions can increase the propulsion system energy consumption by up to 35% and could triple the auxiliary's energy consumption when compared to standard traffic conditions. Moreover, the impact of weather conditions on BEB energy consumption is evaluated. Extreme weather conditions can double the bus energy consumption when compared to moderate weather conditions, which, therefore, reduces its driving range significantly.

The presented comprehensive energy analysis helps in determining the battery size of a BEB based on the energy needs of its energy-systems for the given bus operating conditions and the estimated traveled distance before the batteries are being recharged. Therefore, this study gives insights on the interdependency between the battery size and the charging strategy for avoiding schedule disruptions and for minimizing the size of the battery. For example, BEBs presenting high energy consumption during the operation may require either a large battery capacity with a slow-charge strategy overnight in the bus depot or a reduced battery capacity with frequent and rapid charging during the day to cope with the defined bus schedule.

The presented model could be easily replicated and adapted for any BEB configuration, therefore, allowing the assessment of its total energy consumption under the operating conditions. The multi-physical presented model can be used to simulate the BEB energy consumption in real-time operation, over the entire defined bus schedule for example. Real-time simulations are useful to precisely monitor the battery SOC over the bus schedule, which affects its charging strategy as it considers real and dynamic operating conditions. In addition, real-time simulations of BEBs are extremely useful when the system under study is an entire BEB line composed of many buses interacting with each other in terms of sharing chargers and charging stations. The authors will present in future work the interdependencies between the battery size and the charging strategy and their impact on the cost and operation of BEBs. In addition, the authors will introduce a BEB line model based on the proposed BEB energy model that allows the real-time simulation of the BEBs under real and dynamic operating conditions.

5. References

[1] Emissions from heavy-duty vehicles 2018. https://www.iea.org/tcep/transport/trucks/ (accessed October 8, 2018).

[2] Transport emissions | Climate Action 2016. https://ec.europa.eu/clima/policies/transport_en (accessed October 8, 2018).

[3] Corazza MV, Guida U, Musso A, Tozzi M. A European vision for more environmentally friendly buses. Transp Res Part D Transp Environ 2016;45:48–63. doi:10.1016/j.trd.2015.04.001.

[4] Tong F, Hendrickson C, Biehler A, Jaramillo P, Seki S. Life cycle ownership cost and environmental externality of alternative fuel options for transit buses. Transp Res Part D Transp Environ 2017;57:287–302. doi:10.1016/j.trd.2017.09.023.

[5] Miles J, Potter S. Research in Transportation Economics Developing a viable electric bus service : The Milton Keynes demonstration project. Res Transp Econ 2014;48:357–63. doi:10.1016/j.retrec.2014.09.063.

[6] Offer GJ, Howey D, Contestabile M, Clague R, Brandon NP. Comparative analysis of battery electric , hydrogen fuel cell and hybrid vehicles in a future sustainable road transport system. Energy Policy 2010;38:24–9. doi:10.1016/j.enpol.2009.08.040.

[7] Haddad M, Mansour C, Diab J. System dynamics modeling for mitigating energy use and CO2 emissions of freight transport in Lebanon. Proc. Int. Conf. Ind. Eng. Oper. Manag.,

2019, p. 644–54.

[8] Lajunen A. Energy consumption and cost-benefit analysis of hybrid and electric city buses. Transp Res Part C Emerg Technol 2014;38:1–15. doi:10.1016/j.trc.2013.10.008.

[9] Botsford C, Szczepanek A. Fast Charging vs . Slow Charging : Pros and cons for the New Age of Electric Vehicles. Evs24 2009:1–9.

[10] Jung G, Song B, Shin S, Lee S, Shin J, Kim Y, et al. High efficient inductive power supply and pickup system for on-line electric bus. 2012 IEEE Int Electr Veh Conf IEVC 2012 2012. doi:10.1109/IEVC.2012.6183263.

[11] Xu Y, Gbologah FE, Lee DY, Liu H, Rodgers MO, Guensler RL. Assessment of alternative fuel and powertrain transit bus options using real-world operations data: Life-cycle fuel and emissions modeling. Appl Energy 2015;154:143–59. doi:10.1016/j.apenergy.2015.04.112.

[12] Halmeaho T, Rahkola P, Tammi K, Pippuri J, Pellikka A-P, Manninen A, et al. Experimental validation of electric bus powertrain model under city driving cycles. IET Electr Syst Transp 2017;7:74–83. doi:10.1049/iet-est.2016.0028.

[13] Delgado OF, Clark NN, Thompson GJ. Modeling Transit Bus Fuel Consumption on the Basis of Cycle Properties. J Air Waste Manag Assoc 2011;61:443–52. doi:10.3155/1047-3289.61.4.443.

[14] Mansour C, Haddad M, Zgheib E. Assessing consumption , emissions and costs of electri fi ed vehicles under real driving conditions in a developing country with an inadequate road transport system. Transp Res Part D Transp Environ 2018;63:498–513. doi:10.1016/j.trd.2018.06.012.

[15] Gao Z, Laclair T, Ou S, Huff S, Wu G, Hao P, et al. Evaluation of electric vehicle component performance over eco-driving cycles. Energy 2019;172:823–39. doi:10.1016/j.energy.2019.02.017.

[16] Perrotta D, Teixeira A, Silva H, Ribeiro B. Electrical Bus Performance Modeling for Urban Environments. SAE Int J Altern Powertrains 2012:34–45. doi:10.4271/2012-01-0200.

[17] Mallon KR, Assadian F, Fu B. Analysis of on-board photovoltaics for a battery electric bus and their impact on battery lifespan. Energies 2017;10. doi:10.3390/en10070943.

[18] Suh IS, Lee M, Kim J, Oh ST, Won JP. Design and experimental analysis of an efficient HVAC (heating, ventilation, air-conditioning) system on an electric bus with dynamic on-road wireless charging. Energy 2015;81:262–73. doi:10.1016/j.energy.2014.12.038.

[19] Lajunen A. Energy Efficiency and Performance of Cabin Thermal Management in Electric Vehicles. SAE Tech Pap 2017. doi:10.4271/2017-01-0192.Copyright.

[20] Fayazbakhsh MA, Bahrami M. Comprehensive Modeling of Vehicle Air Conditioning Loads Using Heat Balance Method. SAE Tech Pap 2013. doi:10.4271/2013-01-1507.

[21] Brèque F, Nemer M. Cabin Thermal Needs: Modeling and Assumption Analysis. Proc. 12th Int. Model. Conf., Prague: 2017, p. 771–81.

doi:http://dx.doi.org/10.3384/ecp17132771.

[22] Bréque F. Etude et amélioration d'une pompe à chaleur pour véhicule électrique en conditions de givrage. PSL Research University - Mines Paristech, 2017.

[23] Lajuneni A, Kalttonen A. Investigation of Thermal Energy Losses in the Powertrain of an Electric City Bus. 2015 IEEE Transp. Electrif. Conf. Expo, 2015. doi:10.1109/ITEC.2015.7165776.

[24] Yan M, He H, Sun C, Jia H, Li M. Stochastic Dynamic Programming of Air Conditioning System under Time-varying Passenger Condition for Electric Bus. Energy Procedia 2016;104:360–5. doi:10.1016/j.egypro.2016.12.061.

[25] Göhlich D, Ly T, Kunith A, Jefferies D. Economic assessment of different air-conditioning and heating systems for electric city buses based on comprehensive energetic simulations. EVS28 Int. Electr. Veh. Symp. Exhib., 2015, p. 1–9.

[26] Mansour C, Bou Nader W, Breque F, Haddad M. Assessing additional fuel consumption from cabin thermal comfort and auxiliary needs on the worldwide harmonized light vehicles test cycle. Transp Res Part D Transp Environ 2018;62:139–51. doi:10.1016/j.trd.2018.02.012.

[27] Pettersson N, Johansson KH. Modelling and control of auxiliary loads in heavy vehicles. Int J Control 2007;79:479–95. doi:10.1080/00207170600587333.

[28] Göhlich D, Fay TA, Jefferies D, Lauth E, Kunith A, Zhang X. Design of urban electric bus systems. Des Sci 2018;4:1–28. doi:10.1017/dsj.2018.10.

[29] Göhlich D, Fay TA, Jefferies D, Lauth E, Kunith A, Zhang X. Design of urban electric bus systems. Des Sci 2018;4:1–28. doi:10.1017/dsj.2018.10.

[30] Https://www.3ds.com/products-services/catia/produc. Dymola 2019.

[31] Guzzella L, Sciarretta A. Vehicle Propulsion Systems. Berlin, Heidelberg: Springer Berlin Heidelberg; 2013. doi:10.1007/978-3-642-35913-2.

[32] Markel T, Brooker A, Hendricks T, Johnson V, Kelly K, Kramer B, et al. ADVISOR: a systems analysis tool for advanced vehicle modeling. J Power Sources 2003.

[33] Nanophosphate® High Power Lithium Ion Cell AHR32113M1Ultra-B 2011. https://www.buya123products.com/uploads/vipcase/b1f71087d0071f682891c64c9540ff58.pdf.

[34] Rothgang S, Rogge M, Becker J, Sauer DU. Battery Design for Successful Electrification in Public Transport 2015:6715–37. doi:10.3390/en8076715.

[35] He H, Xiong R, Fan J. Evaluation of lithium-ion battery equivalent circuit models for state of charge estimation by an experimental approach. Energies 2011;4:582–98. doi:10.3390/en4040582.

[36] Bou Nader WS, Mansour CJ, Nemer MG, Guezet OM. Exergo-technological explicit methodology for gas-turbine system optimization of series hybrid electric vehicles. Proc Inst Mech Eng Part D J Automob Eng 2018;232:1323–38.

doi:10.1177/0954407017728849.

[37] Mansour CJ. Trip-based optimization methodology for a rule-based energy management strategy using a global optimization routine: The case of the Prius plug-in hybrid electric vehicle. Proc Inst Mech Eng Part D J Automob Eng 2016;230:1529–45. doi:10.1177/0954407015616272.

[38] Park C, Jaura AK. Dynamic Thermal Model of Li-Ion Battery for Predictive Behavior in Hybrid and Fuel Cell Vehicles. Futur. Transp. Technol. Conf., California: 2003.

[39] Lin X, Perez HE, Siegel JB, Stefanopoulou AG, Li Y, Anderson RD, et al. Online Parameterization of Lumped Thermal Dynamics in Cylindrical Lithium Ion Batteries for Core Temperature Estimation and Health Monitoring. IEEE Trans Control Syst Technol 2013;21:1745–55. doi:10.1109/TCST.2012.2217143.

[40] Lin X, Perez HE, Mohan S, Siegel JB, Stefanopoulou AG, Ding Y, et al. A lumped-parameter electro-thermal model for cylindrical batteries. J Power Sources 2014;257:1–11. doi:10.1016/j.jpowsour.2014.01.097.

[41] Thomas KE, Newman J. Thermal Modeling of Porous Insertion Electrodes. J OfThe Electrochem Soc 2003:176–92. doi:10.1149/1.1531194.

[42] Kim GH, Pesaran A. Battery Thermal Management System Design Modeling 2006.

[43] Axial fans FB 2012. https://termocom.com.ua/images/catalogs/Axial_fan_FB.pdf.

[44] Wang Q, Jiang B, Li B, Yan Y. A critical review of thermal management models and solutions of lithium-ion batteries for the development of pure electric vehicles. Renew Sustain Energy Rev 2016;64:106–28. doi:10.1016/j.rser.2016.05.033.

[45] APTA Bus Procurement Guidelines (June 2013). 2013.

[46] Liebers M, Tretsiak D, Klement S, Bäker B, Wiemann P. Using Air Walls for the Reduction of Open-Door Heat Losses in Buses. SAE Int J ACommercial Veh 2018. doi:10.4271/2017-01-9179.

[47] Al Haddad R, Basma HM, Mansour C. Analysis of heat pump performance in battery electric buses. 32nd Int. Conf. Effic. Cost, Optim. Simul. Environ. Impact Energy Syst. Jun 2019, Wroclaw, Poland., Wroclaw, Poland: 2019.

[48] Andersson C. On auxiliary systems in commercial vehicles. Lund University, 2004.

6. Figures Caption Text:

Figure Number and Caption	Figure Size (Image Width)
Figure 1: BEB components configuration	2 Columns
Figure 2: Battery empirical data	1 Column

Figure 3: Schematic of the battery pack	2 Columns
Figure 4: Electric Machine efficiency map	1 Column
Figure 5: HVAC Unit Scheme	2 Columns
Figure 6: Propulsion system energy consumption at different driving conditions	1.5 Columns
Figure 7: Auxiliaries' energy consumption at different driving conditions	1.5 Columns
Figure 8: HVAC unit average electric power consumption at different external temperatures	1 Column
Figure 9: BTMS average electric power demand at different external temperatures	1 Column
Figure 10: HVAC unit average electric power demand at different passengers' load	1 Column
Figure 11: Energy consumption/power demand of each energy system at the varying operating	2 Columns
Figure 12: Variation of BEB energy consumption at different operating conditions, (a) maximum occupancy, (b) 50% occupancy, (c) 10% occupancy	2 Columns

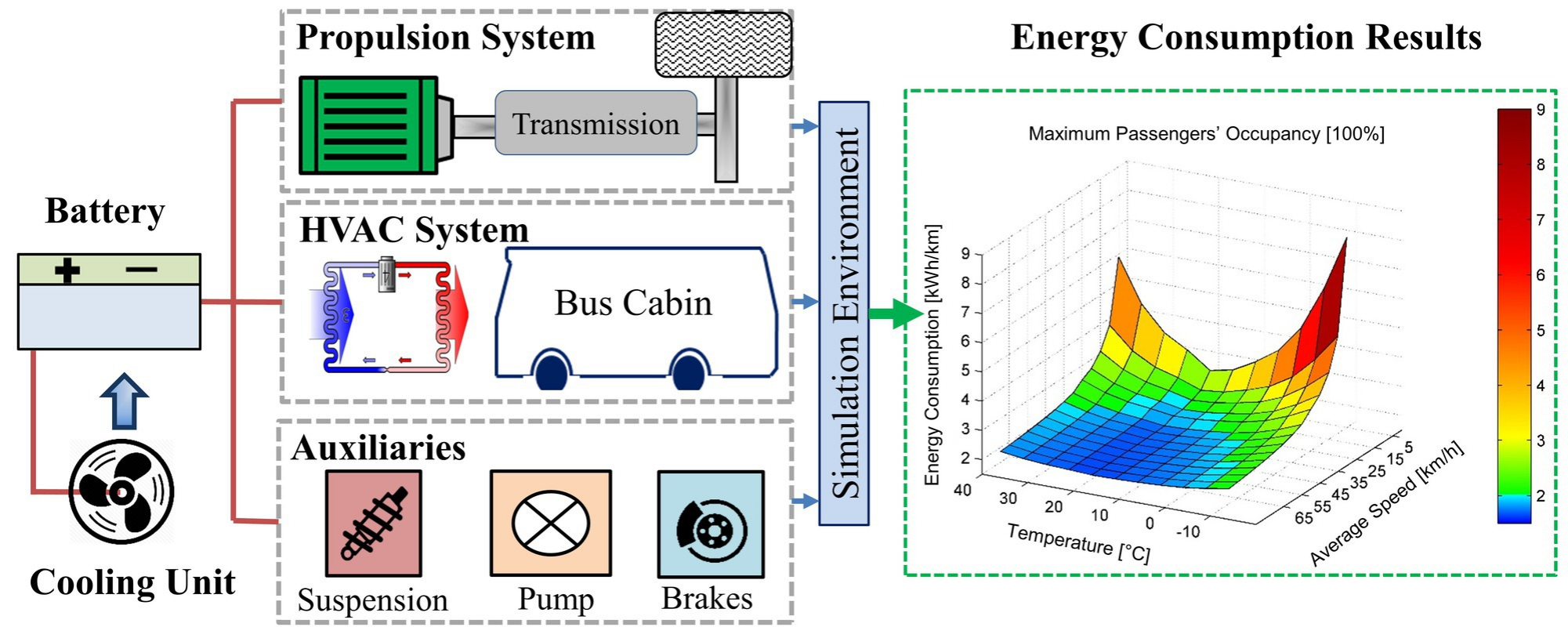
Propulsion System
Transmission
HVAC System
Bus Cabin
Auxiliaries
Suspension
Pump
Brakes
Battery
Cooling Unit
Simulation Environment
Energy Consumption Results
Maximum Passengers' Occupancy [100%]
Energy Consumption [kWh/km]
Temperature [°C]
Average Speed [km/h]